

# BCS-BEC Crossover and Thermodynamics in Asymmetric Nuclear Matter with Pairings in Isospin $I = 0$ and $I = 1$ Channels

Shijun Mao<sup>1</sup>, Xuguang Huang<sup>1,2</sup> and Pengfei Zhuang<sup>1</sup>

<sup>1</sup>*Physics Department, Tsinghua University, Beijing 100084, China*

<sup>2</sup>*Frankfurt Institute for Advanced Studies and Institute for Theoretical Physics, Frankfurt University, Frankfurt am Main D-60438, Germany*

(Dated: February 12, 2022)

The BCS-BEC crossover and phase diagram for asymmetric nuclear superfluid with pairings in isospin  $I = 0$  and  $I = 1$  channels are investigated at mean field level, by using a density dependent nucleon-nucleon potential. Induced by the in-medium nucleon mass and density dependent coupling constants, neutron-proton Cooper pairs could be in BEC state at sufficiently low density, but there is no chance for the BEC formation of neutron-neutron and proton-proton pairs at any density and asymmetry. We calculate the phase diagram in asymmetry-temperature plane for weakly interacting nuclear superfluid, and find that including the  $I = 1$  channel changes significantly the phase structure at low temperature. There appears a new phase with both  $I = 0$  and  $I = 1$  pairings at low temperature and low asymmetry, and the gapless state in any phase with  $I = 1$  pairing is washed out and all excited nucleons are fully gapped.

PACS numbers: 21.60.-n, 26.60.+c, 74.20.-z

## I. INTRODUCTION

As it is well-known, due to the condensate of nucleon-nucleon (NN) Cooper pairs at sufficiently low temperature, a nucleon many-body system, such as a large  $N$  nucleus or bulk nuclear matter in neutron stars, will be in superfluid state with many various interesting phenomena, like the properties of medium-mass  $N \approx Z$  nuclei produced at the radioactive nuclear beam facilities [1, 2], the deuteron formation in medium-energy heavy ion collisions [3], and the equation of state of neutron stars [4, 5]. Considering the spin and isospin degrees of freedom, the NN Cooper pairs should have rich inner structure and hence different phase diagrams.

Recently, two research directions in the study of nuclear matter receive more attention. One is the BCS-BEC crossover [3, 6–13]. When nuclear density decreases, the weakly correlated NN BCS state at high density may go over to the BEC superfluid of NN bound state at lower density. Although the BCS and BEC limits are physically quite different, the change from BCS to BEC was found to be smooth [14–16]. For neutron-proton ( $np$ ) pairs in  ${}^3S_1 - {}^3D_1$  channel, the chemical potential changes sign at a critical density which can be regarded as a criterion of the formation of BEC and finally approaches to a half of the deuteron binding energy at low density limit [3, 7]. Recently, the possible BCS-BEC crossover of neutron-neutron ( $nn$ ) pairs in  ${}^1S_0$  channel was studied by examining the spatial structure of two correlated neutrons [11, 13] and the density and spin correlation functions [10]. It was found that a di-neutron BEC state can be formed in symmetric nuclear matter at very low neutron density. However, when the degree of isospin asymmetry is high, there is no such a BEC state in the whole density region.

The other direction is the possible phase transition induced by the mismatch between neutron and proton Fermi surfaces [17–22]. When the isospin asymmetry becomes sufficiently high, namely when the mismatch is comparable with the  $np$  pairing gap, the pairing will be suppressed. A phase transition from the BCS state to normal nuclear fluid is expected at a

critical isospin asymmetry. However, for an asymmetric system, besides the BCS state, some other superfluid states are suggested in condensed matter and nuclear matter, such as the Sarma phase [23] or breached pairing phase [24] where the superfluid component is breached by the normal component in momentum space, the Fulde-Ferrel-Larkin-Ovchinnikov (FFLO) phase [25] where a Cooper pair has a total momentum and the translational symmetry is spontaneously broken, the deformed Fermi surface phase [26, 27] where the Fermi surfaces of the two species are deformed into ellipsoidal shape and cross to each other so that Cooper pairs with zero total momentum could form at the cross node, and the phase separation (PS) in real space [28, 29] where the normal and superfluid components are inhomogeneously mixed.

Since nucleons could form Cooper pairs in both isospin singlet and triplet channels, it is natural to ask a question of how the competition between the isospin  $I = 0$  pairing, namely the  $np$  pairing, and  $I = 1$  pairing, namely the  $nn$  and  $pp$  pairing, affects the BCS-BEC crossover and thermodynamics of nuclear superfluid. To have an insight into this question, we perform in this paper a mean field analysis for the asymmetric nuclear matter with the above two kinds of pairings. The mean field approximation is an effective and successful treatment at low temperature or for weakly correlated systems. At high temperature or for strongly coupled systems, pair fluctuations may become significant [15]. We will restrict our study on the BCS-BEC crossover at zero temperature and the thermodynamics at high density. To simplify numerical calculations, We use a density dependent contact potential to describe the NN interaction.

The paper is organized as follows. We present the mean field formalism for a general asymmetric nuclear matter with isospin  $I = 0$  and  $I = 1$  pairings in Section II. The possibility of BCS-BEC crossover for the two channels is investigated in Section III, and the significant change in the phase structure of weakly interacting nuclear superfluid at finite temperature is discussed in Section IV. We summarize in section V.

## II. MEAN FIELD FORMALISM

We adopt the density dependent contact interaction (DDCI) developed by Gorrido et. al. [30] to model the NN potential, due to its simplicity and validity in pairing problem. For the purpose of getting qualitative conclusions which should not be sensitive to the details of the interacting dynamics, the DDCI potential is acceptable. The potential is of the form

$$V(\mathbf{x}, \mathbf{x}') = v \left[ 1 - \eta \left( \frac{\rho((\mathbf{x} + \mathbf{x}')/2)}{\rho_0} \right)^\gamma \right] \delta(\mathbf{x} - \mathbf{x}'), \quad (1)$$

where  $v, \eta$  and  $\gamma$  are three adjustable parameters,  $\rho(\mathbf{x}) = \rho_n(\mathbf{x}) + \rho_p(\mathbf{x})$  is the nuclear density. Taking suitable values of the parameters, one can reproduce [30] the pairing gap  $\Delta(k_F)$  as a function of the Fermi momentum  $k_F = (3\pi^2\rho/2)^{1/3}$  in the channels  $L = 0, I = 1, I_z = \pm 1, S = 0$  and  $L = 0, I = 0, S = 1, S_z = 0$ . We will choose in the following numerical calculations the parameters [30]  $\eta = 0.45, \gamma = 0.47, v = -481 \text{ MeVfm}^3$  in the  $I = 1$  channel and  $\eta = 0, v = -530 \text{ MeVfm}^3$  in the  $I = 0$  channel and the energy cutoff  $\epsilon_c = 60 \text{ MeV}$  in both channels to regularize the integration. With these parameters one must use a density-dependent effective nucleon mass  $m(\rho)$  [30], corresponding to the Gogny interaction [31],

$$\frac{m_0}{m(\rho)} = 1 + \frac{m_0 k_F}{2 \sqrt{\pi}} \sum_{c=1}^2 [W_c + 2(B_c - H_c) - 4M_c] \times \mu_c^3 e^{-x_c} \left[ \frac{\cosh x_c}{x_c} - \frac{\sinh x_c}{x_c^2} \right] \quad (2)$$

with  $x_c = k_F^2 \mu_c^2 / 2$ , where  $m_0 = 939 \text{ MeV}$  is the nucleon mass in vacuum, and  $\mu_c, W_c, B_c, H_c, M_c$  are parameters by fitting the Gogny force D1 [32, 33], their values are listed in Table I. As shown in Fig. 1, the medium effect suppresses the nucleon mass.

TABLE I: Parameters in the effective nucleon mass (2) by fitting the Gogny interaction D1 [32, 33].

c	$\mu_c$ [fm]	$W_c$ [MeV]	$B_c$ [MeV]	$H_c$ [MeV]	$M_c$ [MeV]
1	0.7	-402.4	-100.0	-496.2	-23.56
2	1.2	-21.30	-11.77	37.27	-68.81

For a uniform nuclear system, the nuclear density  $\rho$  is independent of  $\mathbf{x}$ , and the DDCI potential is simplified to the form of

$$V_I(\mathbf{x} - \mathbf{x}') = g_I \delta(\mathbf{x} - \mathbf{x}') \quad (3)$$

with the effective coupling constant

$$g_I = v_I [1 - \eta_I (\rho/\rho_0)^{\gamma_I}], \quad (4)$$

where  $I = 0, 1$  denote the isospin of pairs.

The uniform nuclear system with the two-body interacting potential  $V_I(\mathbf{x} - \mathbf{x}')$  and chemical potentials  $\mu_n$  and  $\mu_p$  for neutrons and protons is controlled by the Lagrangian density

$$\begin{aligned} \hat{\mathcal{L}} &= \sum_{\sigma=\uparrow,\downarrow} \left[ \hat{p}_\sigma^\dagger(\mathbf{x}) \left( -\frac{\partial}{\partial \tau} + \frac{\nabla^2}{2m} + \mu_p \right) \hat{p}_\sigma(\mathbf{x}) + \hat{n}_\sigma^\dagger(\mathbf{x}) \left( -\frac{\partial}{\partial \tau} + \frac{\nabla^2}{2m} + \mu_n \right) \hat{n}_\sigma(\mathbf{x}) \right] \\ &\quad - \int d^3 \mathbf{x}' V_1(\mathbf{x} - \mathbf{x}') \left[ \hat{n}_\uparrow^\dagger(\mathbf{x}) \hat{n}_\downarrow^\dagger(\mathbf{x}') \hat{n}_\downarrow(\mathbf{x}') \hat{n}_\uparrow(\mathbf{x}) + \hat{p}_\uparrow^\dagger(\mathbf{x}) \hat{p}_\downarrow^\dagger(\mathbf{x}') \hat{p}_\downarrow(\mathbf{x}') \hat{p}_\uparrow(\mathbf{x}) \right] \\ &\quad - \frac{1}{2} \int d^3 \mathbf{x}' V_0(\mathbf{x} - \mathbf{x}') \left[ \hat{n}_\uparrow^\dagger(\mathbf{x}) \hat{p}_\downarrow^\dagger(\mathbf{x}') - \hat{p}_\uparrow^\dagger(\mathbf{x}) \hat{n}_\downarrow^\dagger(\mathbf{x}') \right] \left[ \hat{p}_\downarrow(\mathbf{x}') \hat{n}_\uparrow(\mathbf{x}) - \hat{n}_\downarrow(\mathbf{x}') \hat{p}_\uparrow(\mathbf{x}) \right] \\ &= \sum_{\sigma=\uparrow,\downarrow} \left[ \hat{p}_\sigma^\dagger(\mathbf{x}) \left( -\frac{\partial}{\partial \tau} + \frac{\nabla^2}{2m} + \mu_p \right) \hat{p}_\sigma(\mathbf{x}) + \hat{n}_\sigma^\dagger(\mathbf{x}) \left( -\frac{\partial}{\partial \tau} + \frac{\nabla^2}{2m} + \mu_n \right) \hat{n}_\sigma(\mathbf{x}) \right] \\ &\quad - g_1 \left( \hat{n}_\uparrow^\dagger(\mathbf{x}) \hat{n}_\downarrow^\dagger(\mathbf{x}) \hat{n}_\downarrow(\mathbf{x}) \hat{n}_\uparrow(\mathbf{x}) + \hat{p}_\uparrow^\dagger(\mathbf{x}) \hat{p}_\downarrow^\dagger(\mathbf{x}) \hat{p}_\downarrow(\mathbf{x}) \hat{p}_\uparrow(\mathbf{x}) \right) \\ &\quad - \frac{1}{2} g_0 \left( \hat{n}_\uparrow^\dagger(\mathbf{x}) \hat{p}_\downarrow^\dagger(\mathbf{x}) - \hat{p}_\uparrow^\dagger(\mathbf{x}) \hat{n}_\downarrow^\dagger(\mathbf{x}) \right) \left( \hat{p}_\downarrow(\mathbf{x}) \hat{n}_\uparrow(\mathbf{x}) - \hat{n}_\downarrow(\mathbf{x}) \hat{p}_\uparrow(\mathbf{x}) \right), \quad (5) \end{aligned}$$

where  $\hat{n}_\sigma$  and  $\hat{p}_\sigma$  are neutron and proton field operators with spin  $\sigma$ . We introduce the Cooper pair operators  $\hat{\Delta}_{np}(\mathbf{x}) = -(g_0/2)(\hat{p}_\downarrow(\mathbf{x})\hat{n}_\uparrow(\mathbf{x}) - \hat{n}_\downarrow(\mathbf{x})\hat{p}_\uparrow(\mathbf{x})) = \hat{\Delta}_{np}^*(\mathbf{x})$ ,  $\hat{\Delta}_{nn}(\mathbf{x}) = -g_1\hat{n}_\downarrow(\mathbf{x})\hat{n}_\uparrow(\mathbf{x}) = \hat{\Delta}_{nn}^*(\mathbf{x})$  and  $\hat{\Delta}_{pp}(\mathbf{x}) = -g_1\hat{p}_\downarrow(\mathbf{x})\hat{p}_\uparrow(\mathbf{x}) = \hat{\Delta}_{pp}^*(\mathbf{x})$ , corresponding to the channels  $L = 0, I = 0, S = 1, S_z = 0$  and  $L = 0, I = 1, I_z = \pm 1, S = 0$ , and keep only their condensates  $\langle \hat{\Delta}_{np}(\mathbf{x}) \rangle$ ,  $\langle \hat{\Delta}_{nn}(\mathbf{x}) \rangle$  and  $\langle \hat{\Delta}_{pp}(\mathbf{x}) \rangle$  in the Lagrangian in mean field approxima-

tion. To incorporate the FFLO state into our study, we assume the following forms of the condensates,  $\langle \hat{\Delta}_{np}(\mathbf{x}) \rangle = \Delta_{np} e^{i(\mathbf{q}_n + \mathbf{q}_p) \cdot \mathbf{x}}$ ,  $\langle \hat{\Delta}_{nn}(\mathbf{x}) \rangle = \Delta_{nn} e^{2i\mathbf{q}_n \cdot \mathbf{x}}$  and  $\langle \hat{\Delta}_{pp}(\mathbf{x}) \rangle = \Delta_{pp} e^{2i\mathbf{q}_p \cdot \mathbf{x}}$ , where  $\Delta_{np}$ ,  $\Delta_{nn}$  and  $\Delta_{pp}$  are constants and can be assumed to be real numbers, and  $\mathbf{q}_n$  and  $\mathbf{q}_p$  are the pair momenta. Obviously, the translational symmetry and rotational symmetry in the FFLO state are spontaneously broken. Note that, for the sake of simplicity, the FFLO state we considered here is its simplest pattern, namely the single plane

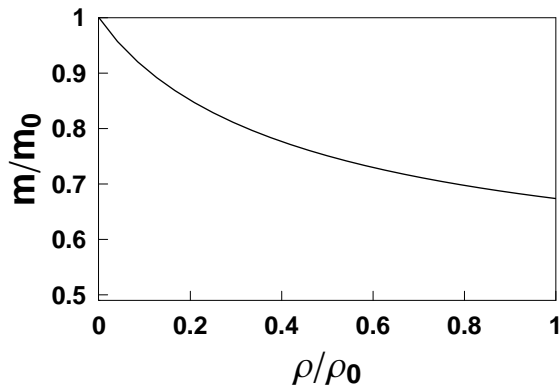


FIG. 1: The effective nucleon mass as a function of nuclear density, calculated from the Gogny force D1.  $m_0$  and  $\rho_0$  are, respectively, nucleon mass in vacuum and normal nuclear density.

wave FFLO state or the so-called FF state.

The partition function  $Z$  which is the key quantity of a thermodynamic system can be calculated by path integral,

$$Z = \Pi_\sigma \int [d\hat{n}_\sigma][d\hat{p}_\sigma][d\hat{n}_\sigma^\dagger][d\hat{p}_\sigma^\dagger] \exp \left( \int_0^\beta d\tau \int d^3\mathbf{x} \hat{\mathcal{L}} \right). \quad (6)$$

By performing a gauge transformation for the nucleon fields  $\tilde{n}_\sigma = e^{-i\mathbf{q}_n \cdot \mathbf{x}} \hat{n}_\sigma$  and  $\tilde{p}_\sigma = e^{-i\mathbf{q}_p \cdot \mathbf{x}} \hat{p}_\sigma$  which keeps the functional measure in Eq.(6) invariant, the path integral over  $\tilde{n}_\sigma$  and  $\tilde{p}_\sigma$  can be easily done and we obtain the mean field thermodynamic potential

$$\begin{aligned} \Omega &= -\frac{T}{V} \ln Z \\ &= -\frac{2\Delta_{np}^2}{g_0} - \frac{\Delta_{nn}^2 + \Delta_{pp}^2}{g_1} \\ &\quad - T \sum_\nu \int \frac{d^3\mathbf{k}}{(2\pi)^3} \text{Tr} \ln G^{-1}(i\omega_\nu, \mathbf{k}), \end{aligned} \quad (7)$$

where  $\omega_\nu = (2\nu + 1)\pi T$  with  $\nu \in \mathbb{Z}$  is the fermion frequency, and  $G$  is the Nambu-Gorkov propagator,

$$G^{-1} = \begin{pmatrix} i\omega_\nu - \epsilon_n^+ & 0 & \Delta_{np} & \Delta_{nn} \\ 0 & i\omega_\nu - \epsilon_p^+ & \Delta_{pp} & -\Delta_{np} \\ \Delta_{np} & \Delta_{pp} & i\omega_\nu + \epsilon_p^- & 0 \\ \Delta_{nn} & -\Delta_{np} & 0 & i\omega_\nu + \epsilon_n^- \end{pmatrix} \quad (8)$$

with the definition  $\epsilon_i^\pm = (\mathbf{k} \pm \mathbf{q}_i)^2 / (2m) - \mu_i$  for  $i = n, p$ . It is worthy noting that, if the relative momentum  $\mathbf{q}_n - \mathbf{q}_p$  is large enough, the uniform superfluid would be unstable due to the stratification of the superfluid components characterized by  $\Delta_{nn}$  and  $\Delta_{pp}$ , in analogous to the multi-component BEC in condensed matter physics. To avoid such a dynamic instability [34], we choose  $\mathbf{q}_n = \mathbf{q}_p = \mathbf{q}$ . After computing the frequency summation and trace in (7), the thermodynamic poten-

tial can be expressed in terms of quasi-particles,

$$\begin{aligned} \Omega &= -\frac{2\Delta_{np}^2}{g_0} - \frac{\Delta_{nn}^2 + \Delta_{pp}^2}{g_1} + \int \frac{d^3\mathbf{k}}{(2\pi)^3} \left[ \epsilon_n^- + \epsilon_p^- \right. \\ &\quad \left. - \sum_{i,j=\pm} \left( \frac{E_j^i}{2} + T \ln \left( 1 + e^{-E_j^i/T} \right) \right) \right], \end{aligned} \quad (9)$$

where  $E_\pm^\mp$  are the quasi-particle energies

$$E_\pm^\mp = \sqrt{\epsilon_\pm^2 + \delta\epsilon^2} \pm \sqrt{\epsilon_\pm^4 + \epsilon_\Delta^4} \mp \delta\epsilon \quad (10)$$

with  $\epsilon_\pm, \delta\epsilon$  and  $\epsilon_\Delta$  defined as

$$\begin{aligned} 2\epsilon_\pm^2 &= \epsilon_n^+ \epsilon_n^- + \Delta_{nn}^2 + \Delta_{np}^2 \pm (\epsilon_p^+ \epsilon_p^- + \Delta_{pp}^2 + \Delta_{np}^2), \\ \delta\epsilon &= (\epsilon_n^+ - \epsilon_n^-) / 2 = (\epsilon_p^+ - \epsilon_p^-) / 2, \\ \epsilon_\Delta^4 &= \Delta_{np}^2 [(\epsilon_n^+ - \epsilon_p^+) (\epsilon_n^- - \epsilon_p^-) + (\Delta_{pp} - \Delta_{nn})^2]. \end{aligned} \quad (11)$$

From the thermodynamic potential, we derive the neutron and proton number densities,

$$\rho_n = -\frac{\partial \Omega}{\partial \mu_n}, \quad \rho_p = -\frac{\partial \Omega}{\partial \mu_p}, \quad (12)$$

or

$$\rho = -\frac{\partial \Omega}{\partial \mu}, \quad \delta\rho = -\frac{\partial \Omega}{\partial \delta\mu}, \quad (13)$$

where  $\mu = (\mu_n + \mu_p) / 2$  is the averaged nucleon chemical potential,  $\delta\mu = (\mu_n - \mu_p) / 2$  the mismatch between  $\mu_n$  and  $\mu_p$ , and  $\delta\rho = \rho_n - \rho_p$  the associated difference in number densities. We will focus on neutron rich nuclear matter with  $\delta\mu > 0$  and  $\delta\rho > 0$ , since it is coincident with the environment of neutron stars and some heavy nuclei. For the sake of convenience, we define the relative density asymmetry  $\alpha = \delta\rho / \rho$ .

The condensates and the FFLO momentum are determined by the gap equations,

$$\frac{\partial \Omega}{\partial \Delta_{np}} = 0, \quad \frac{\partial \Omega}{\partial \Delta_{nn}} = 0, \quad \frac{\partial \Omega}{\partial \Delta_{pp}} = 0, \quad \frac{\partial \Omega}{\partial \mathbf{q}} = 0. \quad (14)$$

With the above coupled number equations (13) and gap equations (14), we can solve the condensates  $\Delta_{np}, \Delta_{nn}, \Delta_{pp}$ , FFLO momentum  $\mathbf{q}$  and chemical potentials  $\mu, \delta\mu$  as functions of temperature  $T$  and densities  $\rho, \delta\rho$ . The ground state of the system is specified by the solution corresponding to the global minimum of the free energy which is related to the thermodynamic potential by a Legendre transformation,  $\mathcal{F} = \Omega + \mu_n \rho_n + \mu_p \rho_p = \Omega + \mu \rho + \delta\mu \delta\rho$ .

### III. BCS-BEC CROSSOVER AT ZERO TEMPERATURE

The mean field approximation has been successfully used to study the BCS-BEC crossover in nuclear matter with isospin  $I = 0$  [3, 6–9] or  $I = 1$  [10–13] pairings. We extend in this section the study to a more general case with both  $I = 0$  and  $I = 1$  pairings. To guarantee the validity of mean field treatment, we focus on the

superfluid at zero temperature. Since the FFLO state is unstable in strong coupling region [35], we will not take into account the FFLO state in the study of BCS-BEC crossover. The temperature effect and the FFLO state will be considered in Section IV.

To examine how the NN correlation changes with nuclear density, we define the normalized Cooper pair wave function as

$$\begin{aligned}\psi_{ij}(\mathbf{r}) &= C \langle BCS | \hat{a}_{i\uparrow}^\dagger(\mathbf{x}) \hat{a}_{j\downarrow}^\dagger(\mathbf{x} + \mathbf{r}) | BCS \rangle \\ &= C' \int \frac{d^3\mathbf{k}}{(2\pi)^3} \psi_{ij}(\mathbf{k}) e^{i\mathbf{k}\cdot\mathbf{r}}\end{aligned}\quad (15)$$

with  $i, j = n, p$ , where  $\hat{a}_{i\sigma}^\dagger$  is the nucleon creation operator, and  $\psi_{ij}(\mathbf{k})$  the wave function in momentum space or the anomalous density

$$\psi_{ij}(\mathbf{k}) = \langle BCS | \hat{a}_{i\uparrow}^\dagger(\mathbf{k}) \hat{a}_{j\downarrow}^\dagger(-\mathbf{k}) | BCS \rangle. \quad (16)$$

The density distribution functions  $n_i(\mathbf{k})$  is defined through

$$n_i(\mathbf{k}) = \frac{1}{2} \sum_{\sigma} \langle BCS | \hat{a}_{i\sigma}^\dagger(\mathbf{k}) \hat{a}_{i\sigma}(\mathbf{k}) | BCS \rangle. \quad (17)$$

In order to describe the BCS-BEC crossover quantitatively, it is convenient to introduce the following characteristic quantities[11, 13]:

1) The distribution function  $r^2 |\psi_{ij}(\mathbf{r})|^2$  which is the probability to find a pair of nucleons  $i$  and  $j$  with distance  $r$  in between. For the BCS-BEC crossover induced by changing coupling constant at fixed density such as in cold atom gas, the probability would distribute in a wide space region in the weakly coupled BCS state but peak sharply at a small  $r$  in the strongly coupled BEC state. However, for nuclear superfluid, the BCS-BEC crossover is induced by changing the nuclear density. The density dependence of any physical quantity of the system is reflected in two aspects: the explicit or direct  $\rho$  dependence through the coupling between the gap and number equations and the indirect  $\rho$  dependence through the effective coupling constant  $g_I(\rho)$  and in-medium nucleon mass  $m(\rho)$ . When the density drops down, the indirect  $\rho$  dependence is the driving force for the crossover from BCS to BEC, but the explicit  $\rho$  dependence makes the system dilute and then slows down or even rejects the crossover. The balance between these two opposite aspects controls the BCS-BEC crossover and will probably change the monotonous shrinking behavior of the probability.

2) The root-mean-square radius of the Cooper pair  $\xi_{ij} = \sqrt{\langle r^2 \rangle_{ij}}$  with  $\langle r^2 \rangle_{ij} = \int d^3\mathbf{r} r^2 |\psi_{ij}(\mathbf{r})|^2$  which characterizes the size of the Cooper pair. When the density is fixed,  $\xi_{ij}$  is expected to be large in the weakly coupled BCS region and small in the strongly coupled BEC region. However, for nuclear superfluid with decreasing nuclear density from BCS to BEC,  $\xi_{ij}$  itself can no longer describe the BCS-BEC crossover. In this case, the BCS and BEC states are defined in the sense of overlapping degree of pair wave functions. At high density the size of a pair can be small but the pairs may overlap strongly, while at low density the size of a pair is probably large but the overlapping of pairs

becomes weak. To represent the density dependence of the overlapping, we can compare  $\xi_{ij}$  with the averaged distance  $d_{ij} = \rho_{ij}^{-1/3}$  between any two nucleons with  $\rho_{np} = \rho/2$ ,  $\rho_{nn} = \rho_n$  and  $\rho_{pp} = \rho_p$ . For  $\xi_{ij} \gg d_{ij}$  the overlapping is strong, and the  $ij$ -pair can be interpreted as an extended BCS pair, while for  $\xi_{ij} \ll d_{ij}$  the overlapping becomes weak, and the pair should be considered as a compact BEC pair, *i.e.*, a boson-like bound state.

3) The probability  $P(d_{ij}) = 4\pi \int_0^{d_{ij}} dr r^2 |\psi_{ij}(\mathbf{r})|^2$  of finding an  $ij$ -Cooper pair within the averaged distance  $d_{ij}$  between the nucleons  $i$  and  $j$ . Note that the probability is density dependent and can be used to describe the overlapping degree of pairs. It should be very close to 1 in the strongly coupled BEC state and clearly less than 1 when the superfluid is in the BCS state.

4) The s-wave scattering length  $a_{ij}$  which relates the coupling constant  $g_I$  to the low energy limit of the T-matrix for nucleons  $i$  and  $j$  in vacuum,

$$\frac{m}{4\pi a_{ij}} = \frac{1}{g_{ij}} + \int \frac{d^3\mathbf{k}}{(2\pi)^3} \frac{1}{2\epsilon_{\mathbf{k}}} \quad (18)$$

with  $\epsilon_{\mathbf{k}} = \mathbf{k}^2/(2m)$  and  $g_{np} = g_0, g_{nn} = g_{pp} = g_1$ . In the BCS region  $a_{ij}$  is negative, representing the attractive interaction between nucleons. However, in the BEC region it should be positive to preserve the stability of the two-body bound state. Therefore, the change of  $a_{ij}$  from negative to positive value can be considered as a signature of the BCS-BEC crossover.

5) The scaled condensate  $\Delta_{ij}/\epsilon_F^{ij}$  with the Fermi energy defined as  $\epsilon_F^{ij} = (k_F^{ij})^2/(2m)$ , where  $k_F^{np} = k_F$ ,  $k_F^{nn} = k_{nF}$  and  $k_F^{pp} = k_{pF}$  are the corresponding Fermi momenta. In the case with only  $I = 0$  pairs, the mean field gap equation and number equation satisfy the so-called universality: The scaled quantities like  $\Delta/\epsilon_F$  and  $\mu/\epsilon_F$  are only functions of the effective coupling  $1/(k_F a)$  [14]. In the strongly coupled BEC region, one should expect a large  $\Delta/\epsilon_F$ , but in the weakly interacting BCS state it will be less than 1. While the universality is explicitly broken in our general case with both  $I = 0$  and  $I = 1$  pairings, we still take the scaled quantities to describe the BCS-BEC crossover.

6) The effective chemical potential  $\mu_{ij}/\epsilon_F^{ij}$  with  $\mu_{np} = \mu, \mu_{nn} = \mu_n$  and  $\mu_{pp} = \mu_p$ . Due to the definition,  $\mu_{ij}/\epsilon_F^{ij}$  is exactly equal to 1 in the BCS limit and the order of 1 in the weakly coupled BCS region. In the case of only one kind of pairs, like symmetric nuclear matter and neutron matter discussed below,  $\mu/\epsilon_F$  is negative in the BEC region, the absolute value  $|\mu/\epsilon_F|$  becomes larger and larger as the system goes deeper and deeper into the BEC region, and  $2\mu$  can be viewed as the binding energy of the bound state in the BEC limit when the system approaches to vanishing density. That is the reason why the change of the sign of  $\mu$  is normally considered as an unambiguous criterion of the formation of BEC, at least at mean field level. However, in general asymmetric nuclear matter with  $np$ ,  $nn$  and  $pp$  pairs, the correlations among different pairs will qualitatively change this conclusion, see the detailed discussion in the following.

### A. Symmetric Nuclear Matter: $\alpha = 0$

Let us first consider the symmetric nuclear matter with  $\delta\rho = 0$ ,  $\delta\mu = 0$  and  $\Delta_{nn} = \Delta_{pp}$ . The number and gap equations in this case are largely simplified as

$$\begin{aligned}\rho_n &= \rho_p = 2 \int \frac{d^3\mathbf{k}}{(2\pi)^3} n(\mathbf{k}), \\ n(\mathbf{k}) &= n_n(\mathbf{k}) = n_p(\mathbf{k}) = \frac{1}{2} \left( 1 - \frac{\epsilon_{\mathbf{k}}}{E_{\mathbf{k}}} \right), \\ \Delta_{np} &= -g_0 \Delta_{np} \int \frac{d^3\mathbf{k}}{(2\pi)^3} \frac{1}{2E_{\mathbf{k}}}, \\ \Delta_{nn} &= \Delta_{pp} = -g_1 \Delta_{nn} \int \frac{d^3\mathbf{k}}{(2\pi)^3} \frac{1}{2E_{\mathbf{k}}},\end{aligned}\quad (19)$$

where  $\epsilon_{\mathbf{k}} = \mathbf{k}^2/(2m) - \mu$  is the particle dispersion relation and  $E_{\mathbf{k}} = \sqrt{\epsilon_{\mathbf{k}}^2 + \Delta_{np}^2 + \Delta_{nn}^2}$  the quasi-particle dispersion. The gap equations have two types of non-trivial solutions  $\Delta_{np} \neq 0, \Delta_{nn} = \Delta_{pp} = 0$  and  $\Delta_{np} = 0, \Delta_{nn} = \Delta_{pp} \neq 0$ . Considering  $|g_0| > |g_1|$  at any density, only the solution with  $\Delta_{np} \neq 0$  corresponds to the ground state. This can also be verified by comparing the free energies for the two solutions. Since there is no experimental evidence for  $np$  pairing at finite nuclear density, it is necessary to note that the condition  $|g_0| > |g_1|$  is in principle an assumption in our treatment. From a more self-consistent Greens function approach [36], the tensor correlations in the  $I = 0$  channel may yield a kind of pair correlation which is different from the one observed in solving gap equations.

To simplify the notation, we write in short  $\epsilon_F = \epsilon_F^{np}$  and  $d = d_{np}$  in the following. Solving the coupled number and gap equations for the  $np$  channel, we obtain the scaled gap  $\Delta_{np}(\rho)/\epsilon_F$  and chemical potential  $\mu(\rho)/\epsilon_F$  as functions of nuclear density.

Defining the anomalous density  $\psi_{np}(\mathbf{k}) = \Delta_{np}/(2E_{\mathbf{k}})$  and substituting it into the number and gap equations give the Schrödinger-like equation

$$\frac{\mathbf{k}^2}{m} \psi_{np}(\mathbf{k}) + (1 - 2n_{\mathbf{k}})g_0 \int \frac{d^3\mathbf{k}'}{(2\pi)^3} \psi_{np}(\mathbf{k}') = 2\mu \psi_{np}(\mathbf{k}) \quad (20)$$

for the anomalous density. In the limit of vanishing density,  $n_{\mathbf{k}} \rightarrow 0$ , the equation goes over into the Schrödinger equation for the  $np$  bound state, and the chemical potential  $2\mu$  plays the role of binding energy. Since such a bound state should be a boson, one expects that, at sufficiently low density and low temperature the symmetric nuclear matter is in the BEC phase.

Making the Fourier transformation of the anomalous density  $\psi_{np}(\mathbf{k})$  which is determined by solving the gap and number equations, we obtain the wave function  $\psi_{np}(\mathbf{r})$  in coordinate space. The behavior of the probability distribution  $r^2|\psi_{np}(\mathbf{r})|^2$  as a function of the relative distance  $r$  between the pair partners is shown in Fig. 2. The spatial extension and profile of the probability depend strongly on the density. Near the normal density, the probability function is spatially extended and behaves like the well-known BCS expression [37]  $\psi_{np}(r) \sim K_0(r/\pi\xi_{np}) \sin(k_F r)/(k_F r)$ . The oscillation induced by the sharp Fermi surface at high density is well-known and called Friedel oscillation [38]

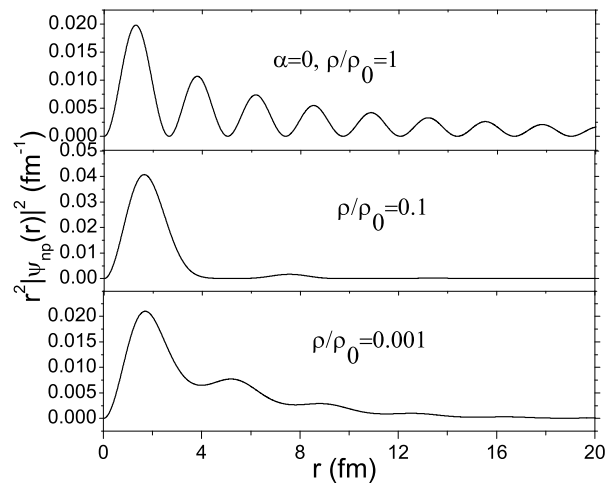


FIG. 2: The probability  $r^2|\psi_{np}(r)|^2$  as a function of the relative distance  $r$  between the paired neutron and proton at different nuclear density  $\rho$  in symmetric nuclear matter.

which is widely discussed in nuclear matter and recently extended to quark matter [39]. The Fermi surface is strictly defined only in normal state without any condensate. In the BCS region at high density, the condensate is small and there is still an approximate Fermi surface. However, in the BEC region at low density, the Fermi surface is already very low and further deformed by the large condensate. The number density as a function of momentum is plotted in Fig. 3. It is clear that the Fermi surface is well-defined only at high density. This is the reason why the Friedel oscillation almost disappears at low density.

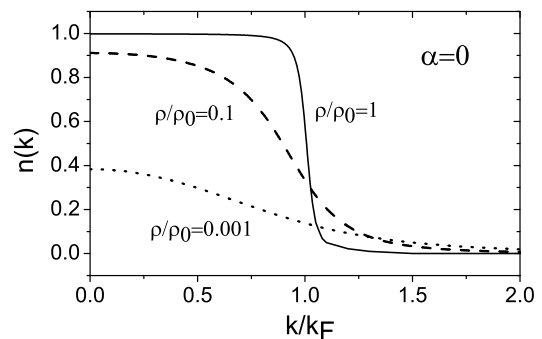


FIG. 3: The nuclear density distribution  $n(k)$  as a function of momentum at fixed nuclear density  $\rho$  in symmetric nuclear matter.  $k_F$  is the Fermi momentum.

It is necessary to note that the probability  $r^2|\psi_{np}(r)|^2$  does not shrink monotonously with decreasing number density, see Fig. 2. For a very dilute system, the two partners of a pair can have a large distance between them, the pair wave function will be spatially extended, and the probability can then distribute in a wide space region. While the strong Friedel oscillation at high density and its weakening at low density can be considered to distinguish the BCS state from the BEC state, the space extension of the probability itself can not be used to characterize the BCS-BEC crossover in

nuclear superfluid.

To clearly describe the BCS-BEC crossover induced by the change in nuclear density, we now calculate the scaled root-mean-square radius  $\xi_{np}/d$ , the scaled chemical potential  $\mu/\epsilon_F$ , the scaled gap parameter  $\Delta_{np}/\epsilon_F$ , the effective scattering length  $1/(k_F a_{np})$  and the probability  $P_{np}(d)$ .  $\xi_{np}/d$  and  $\mu/\epsilon_F$  are presented in Fig. 4 as functions of nuclear density. While  $\xi_{np}$  itself is not a monotonous function of  $\rho$ , the scaled one goes up monotonously with increasing density. The right vertical line at  $\rho/\rho_0 \sim 0.4$  indicates the position of  $\xi_{np}/d = 1$  which can be used to separate the BCS region with sharply increasing  $\xi_{np}/d$  from the region with slightly changing and small  $\xi_{np}/d$ . The scaled chemical potential is 1 in the BCS limit, then drops down with decreasing density, and becomes negative at very small density. The position where  $\mu/\epsilon_F$  approaches to zero is indicated by the left vertical line at  $\rho/\rho_0 \sim 0.003$  which is, from the definition, considered to distinguish the BEC region with negative  $\mu$  from the other region with positive  $\mu$ . Therefore, considering both  $\xi_{np}/d$  and  $\mu/\epsilon_F$ , the BCS and BEC states are, respectively, located at  $\rho/\rho_0 > 0.4$  and  $\rho/\rho_0 < 0.003$ , and the crossover from BCS to BEC is in between the two vertical lines.

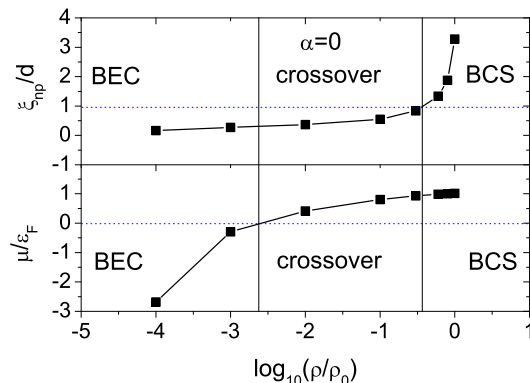


FIG. 4: The scaled root-mean-square radius  $\xi_{np}/d$  and scaled chemical potential  $\mu/\epsilon_F$  as functions of nuclear density in symmetric nuclear matter.  $\epsilon_F$  is the nucleon Fermi energy and  $d$  the averaged distance between two nucleons. The right and left vertical lines which separate the BCS, BEC and crossover regions are, respectively, determined by the conditions  $\xi_{np}/d = 1$  and  $\mu/\epsilon_F = 0$ .

In Fig. 5 we show the scaled condensate  $\Delta_{np}/\epsilon_F$  and the effective s-wave scattering length  $1/(k_F a_{np})$ . Both are monotonous functions of  $\rho$ , while again the gap parameter  $\Delta_{np}$  itself does not behave monotonously. The scaled gap is large at low density and small at high density and approaches to zero in the BCS limit. The effective scattering length drops down with increasing density and becomes negative at high density. The density dependence of  $\Delta_{np}/\epsilon_F$  and  $1/(k_F a_{np})$  agrees well with the normal understanding of both BCS state with small gap and negative scattering length and BEC state with large gap and large and positive scattering length.

The probability  $P_{np}(d)$  of finding a pair with relative distance  $r \leq d$  between the paired neutron and proton is plotted in Fig. 6. Again, while the probability  $P_{np}(r)$  is not a monotonous function of  $\rho$  for fixed  $r$ ,

$P_{np}(d)$  decreases monotonously with increasing density. It approaches to 1 at low density which means strong correlation of pairs in the BEC state and becomes very small at high density which indicates a weak correlation of pairs in the BCS state. The two vertical straight lines in Fig. 5 and Fig. 6 which separate the BCS, BEC and crossover regions are still characterized by the scaled root-mean-square radius and scaled chemical potential. By comparing the above three figures, we can see that  $\xi_{np}/d$ ,  $\mu/\epsilon_F$ ,  $\Delta_{np}/\epsilon_F$ ,  $1/(k_F a_{np})$  and  $P_{np}(d)$  can self-consistently describe the BCS-BEC crossover in symmetric nuclear superfluid.

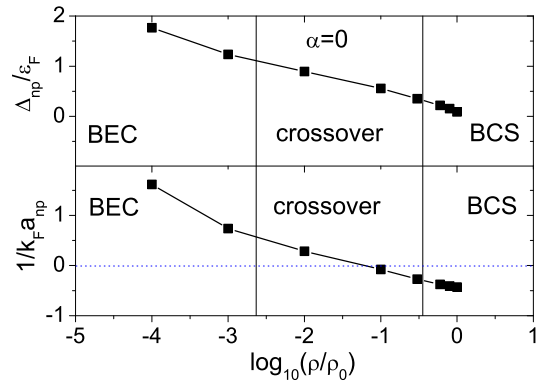


FIG. 5: The scaled condensate  $\Delta_{np}/\epsilon_F$  and effective scattering length  $1/(k_F a_{np})$  as functions of nuclear density in symmetric nuclear matter.  $a_{np}$  is the neutron-proton scattering length.

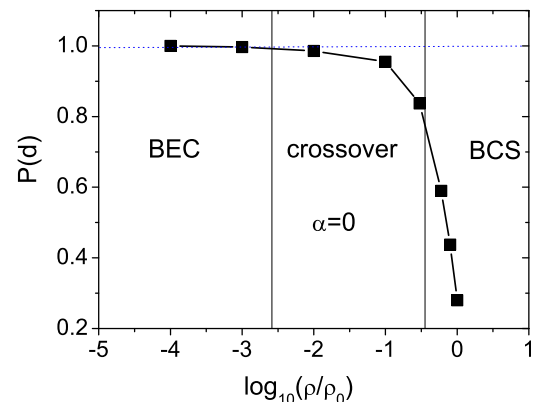


FIG. 6: The probability  $P_{np}(d)$  of finding a  $np$ -pair with relative distance  $r \leq d$  between the paired neutron and proton as a function of nuclear density in symmetric nuclear matter.

## B. Neutron Matter: $\alpha = 1$

Neutron matter, as fully asymmetric nuclear matter, is important for physics of neutron stars. In this case, there are  $\alpha = 1$ ,  $\rho_n = \rho$ ,  $\rho_p = 0$  and  $\Delta_{np} = \Delta_{pp} = 0$ . By solving the coupled number equation and gap equation for  $\rho_n$  and  $\Delta_{nn}$  which are exactly the same as Eq.(19) when we replace  $\epsilon_k$  and  $E_k$

by  $\epsilon_{n\mathbf{k}} = \mathbf{k}^2/(2m) - \mu_n$  and  $E_{n\mathbf{k}} = \sqrt{\epsilon_{n\mathbf{k}}^2 + \Delta_{nn}^2}$ , we obtain the neutron chemical potential  $\mu_n$  and  $nn$  pair condensate  $\Delta_{nn}$  as functions of nuclear density. The anomalous density  $\psi_{nn}(\mathbf{k}) = \Delta_{nn}/(2E_{n\mathbf{k}})$  satisfies the similar Schrödinger-like equation (20), and in the low density limit  $2\mu_n$  plays the role of binding energy of the possible di-neutron bound state.

In comparison with the symmetric nuclear matter, the probability  $r^2|\psi_{nn}(\mathbf{r})|^2$  and the density distribution  $n_n(\mathbf{k})$  at different total number density are very similar to  $r^2|\psi_{np}(\mathbf{r})|^2$  and  $n(\mathbf{k})$  shown in Fig. 2 and Fig. 3, but the scaled root-mean-square radius  $\xi_{nn}/d_{nn}$ , chemical potential  $\mu_n/\epsilon_{nF}$ , gap parameter  $\Delta_{nn}/\epsilon_{nF}$  and the effective scattering length  $1/(k_{nF}a_{nn})$  behave very differently in the low density region. In Fig. 7 and Fig. 8, the vertical straight line located at  $\rho = 0.15\rho_0$  is determined by the condition  $\xi_{nn}/d_{nn} = 1$ , which indicates the BCS region at higher density. However, one can not define the BEC region through the definition  $\mu_n = 0$ , since  $\mu_n$  is always positive in the whole density region, and correspondingly the scaled condensate  $\Delta_{nn}/\epsilon_{nF}$  is still small and the effective scattering length  $1/(k_{nF}a_{nn})$  is still positive at extremely low density. All of these characteristics indicate that no boson degree of freedom emerges in neutron matter at low density.

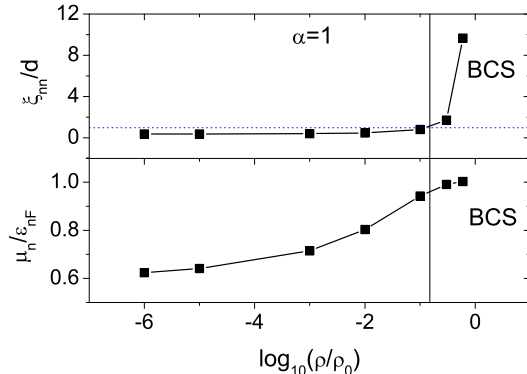


FIG. 7: The scaled root-mean-square radius  $\xi_{nn}/d_{nn}$  and neutron chemical potential  $\mu_n/\epsilon_{nF}$  as functions of nuclear density in neutron matter. The vertical line represents the BCS boundary.  $d_{nn}$  is the averaged distance between two neutrons and  $\epsilon_{nF}$  the neutron Fermi energy.

One can understand the reason why there is no BEC in neutron matter in terms of the density dependent coupling constant  $g_I$  and the Fermi surface  $k_{nF}$ . For the DDCI potential parameters chosen by fitting the pairing gap versus Fermi momentum, the effective coupling in  $I = 1$  channel is weaker than the one in  $I = 0$  channel at any density,  $|g_1(\rho)| < |g_0(\rho)|$ , and on the other hand, the neutron density  $\rho_n = \rho$  in neutron matter is two times the neutron or proton density  $\rho_n = \rho_p = \rho/2$  in symmetric matter. From this comparison, while BEC can form in symmetric nuclear matter, its formation in a dense neutron matter with weak coupling becomes difficult and even impossible. This explains also why the BCS boundary shifts from  $\rho/\rho_0 = 0.4$  in symmetric matter to 0.15 in neutron matter.

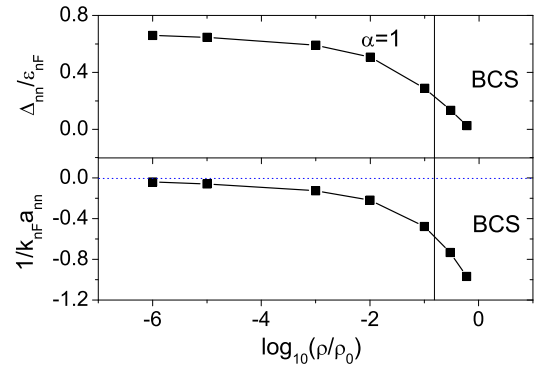


FIG. 8: The scaled condensate  $\Delta_{nn}/\epsilon_{nF}$  and effective scattering length  $1/(k_{nF}a_{nn})$  as functions of nuclear density in neutron matter.  $a_{nn}$  is the neutron-neutron scattering length.

### C. Asymmetric Nuclear Matter: $0 < \alpha < 1$

While only  $np$  condensate in symmetric nuclear matter with  $\alpha = 0$  and  $nn$  condensate in neutron matter with  $\alpha = 1$  can survive, there may exist  $np$ ,  $nn$  and  $pp$  condensates in asymmetric nuclear matter with  $0 < \alpha < 1$ . In this general case, the three condensates  $\Delta_{np}$ ,  $\Delta_{nn}$  and  $\Delta_{pp}$  and the chemical potentials  $\mu$  and  $\delta\mu$  as functions of nuclear density  $\rho$  and asymmetry  $\delta\rho$  are calculated by solving the coupled three gap equations and two number equations, and the ground state of the system is determined by comparing the corresponding free energies.

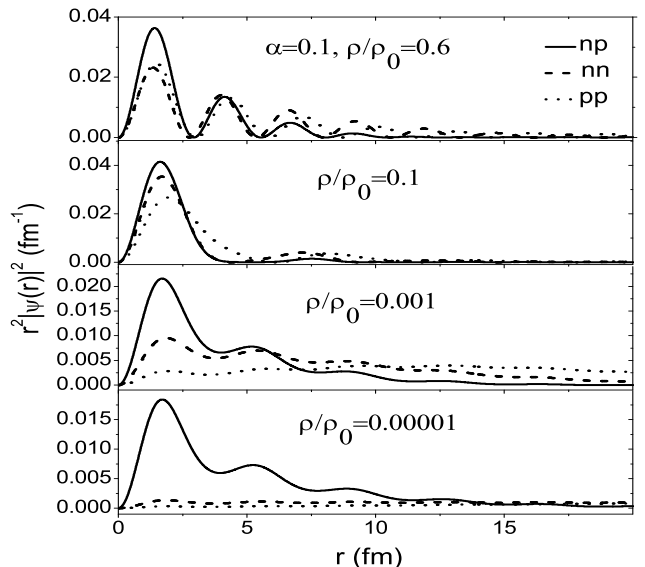


FIG. 9: The probabilities  $r^2|\psi_{np}(r)|^2$ ,  $r^2|\psi_{nn}(r)|^2$  and  $r^2|\psi_{pp}(r)|^2$  as functions of the relative distance  $r$  between the pair partners at different nuclear density in nuclear matter with asymmetry  $\alpha = 0.1$ . At high density  $\rho/\rho_0 = 0.6$ , all the proba-

The three probabilities  $r^2|\psi_{np}(r)|^2$ ,  $r^2|\psi_{nn}(r)|^2$  and  $r^2|\psi_{pp}(r)|^2$  for  $np$ ,  $nn$  and  $pp$  Cooper pairs are shown in Fig. 9 at different nuclear density and fixed asymmetry  $\alpha = 0.1$ . At high density  $\rho/\rho_0 = 0.6$ , all the proba-

bilities are spatially extended with strong Friedel oscillations, indicating that all paired nucleons are weakly correlated and the ground state is in the BCS phase with all three condensates. Similar to the case in symmetric nuclear matter, with decreasing nuclear density  $\rho$  the  $np$  pairing probability shrinks first but slightly expands again at extremely low density. The very surprising feature is that the  $nn$  and  $pp$  pairing probability are spatially expanded in a wide region at low density and even approximately  $r$ -independent at extremely low density. This is a strong hint that there are no BEC states of  $nn$  and  $pp$  pairings in general asymmetric nuclear matter.

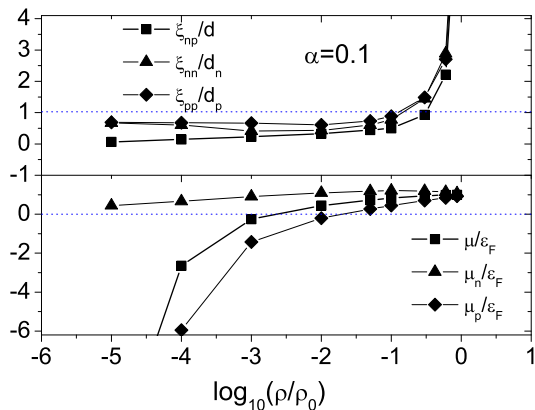


FIG. 10: The scaled root-mean-square radius  $\xi_{ij}/d_{ij}$  and scaled chemical potential  $\mu_i/\epsilon_F$  as functions of nuclear density in nuclear matter with asymmetry  $\alpha = 0.1$ .

To check if the system could reach BEC state at low density, we calculate the scaled root-mean-square radius  $\xi_{ij}/d_{ij}$  and chemical potential  $\mu_i/\epsilon_F$  and show them in Fig. 10 as functions of nuclear density at fixed asymmetry  $\alpha = 0.1$ . The BCS region for the  $ij$  pairing is defined through the condition  $\xi_{ij}/d_{ij} = 1$ . The BCS boundary is roughly at  $\rho/\rho_0 = 0.35$  for  $np$  pairs, 0.14 for  $pp$  pairs and 0.17 for  $nn$  pairs. Below the BCS boundary the system is regarded as a strongly correlated superfluid. As mentioned above, for a system with only one kind of pairings such as symmetric nuclear matter, the strongly correlated system will go into the BEC state when the chemical potential becomes negative. With this judgement, the  $np$  Cooper pairs could reach BEC state at the critical density  $\rho/\rho_0 = 0.002$  where the chemical potential  $\mu$  changes sign. For the  $nn$  pairs, they could never form di-neutron bound state, since the neutron chemical potential is always positive, although it drops down as density decreases. The interesting phenomenon is for the  $pp$  pairing. At  $\rho/\rho_0 = 0.03$ , the proton chemical potential changes sign, even earlier than the change for the  $np$  pairing! Does the negative  $\mu_p$  here mean the formation of  $pp$  BEC state? Is it inconsistent with the flat structure of the probability shown in Fig. 9? To answer this questions, we should note that for a general asymmetric system, the three condensates are strongly coupled and for any anomalous density  $\psi_{ij}(\mathbf{k}) = \Delta_{ij}/(2E_{i\mathbf{k}})$  there is no simple Schrödinger-like equation Eq.(20), and the corresponding chemical potential  $\mu_i$  at low density limit can not

be identified as a half of the binding energy of the di-nucleon bound state. Therefore, there is no longer a definite relation between the sign change of  $\mu_i$  and the BEC formation.

To verify whether the BEC state is reached, we calculate the effective s-wave scattering length  $1/(k_F a_{ij})$ , the scaled condensate  $\Delta_{ij}/\epsilon_{iF}$ , and the probability  $P_{ij}(d)$  as functions of nuclear density at fixed asymmetry  $\alpha = 0.1$ . The results are presented in Fig. 11 and Fig. 12. The scattering length in  $I = 0$  channel changes its sign at about  $\rho/\rho_0 = 0.07$ , but the other two lengths in  $I = 1$  channel remain negative in the whole density region. Correspondingly, the scaled condensate  $\Delta_{np}/\epsilon_F$  becomes much larger than 1 at low density but  $\Delta_{nn}/\epsilon_{nF}$  and  $\Delta_{pp}/\epsilon_{pF}$  are still very small even at extremely low density, and  $P_{np}(d)$  is almost equal to 1 but  $P_{nn}(d)$  and  $P_{pp}(d)$  are clearly less than 1 at low density. Therefore, we can safely say that, the  $np$  BEC state is reached at low density, but there are no  $nn$  and  $pp$  BEC states in general asymmetric nuclear matter.

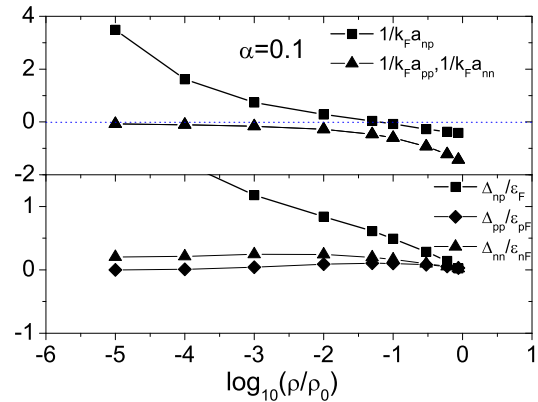


FIG. 11: The scaled condensates  $\Delta_{np}/\epsilon_F$ ,  $\Delta_{nn}/\epsilon_{nF}$ ,  $\Delta_{pp}/\epsilon_{pF}$  and scattering lengths  $1/(k_F a_{np})$ ,  $1/(k_F a_{nn})$ ,  $1/(k_F a_{pp})$  as functions of nuclear density in nuclear matter with asymmetry  $\alpha = 0.1$ .

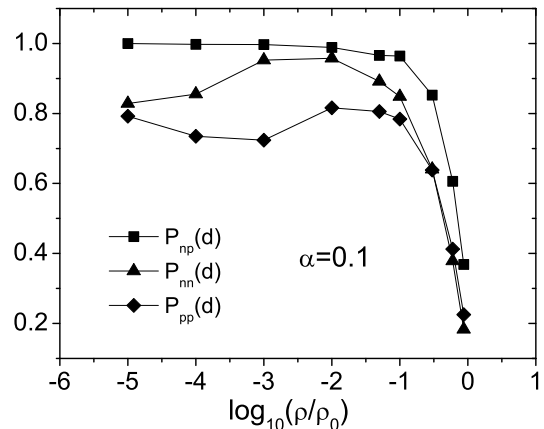


FIG. 12: The probability  $P_{ij}(d)$  as a function of nuclear density in nuclear matter with asymmetry  $\alpha = 0.1$ .

The behavior of the nuclear superfluid in general case with  $0 < \alpha < 1$  is controlled by the two con-



straints  $|g_1(\rho)| < |g_0(\rho)|$  and  $\rho_p = (1 - \alpha)/2\rho < \rho_n = (1 + \alpha)/2\rho < \rho$ . For  $np$  pairings, the effective coupling constant  $g_0$  is density independent in our case, and the crossover from BCS to BEC is characterized by the density dependent nucleon mass (2). For  $nn$  or  $pp$  pairings, the increase of the density leads to a high Fermi surface and then makes the pairing easy, but on the other hand the coupling constant drops down with increasing density. It is the balance between these two effects that the probability  $P_{nn}(d)$  or  $P_{pp}(d)$  is not a monotonous function of density but there exists a valley structure at low density. Since the coupling constant  $g_1$  is the same for  $nn$  and  $pp$  pairings but the Fermi surface for  $nn$  pairing is higher than that for  $pp$  pairing,  $pp$  pairing is most impossible to form a BEC state, that is the reason why the scaled condensate and probability for  $pp$  pairing are less than the corresponding values for  $nn$  pairing, see Fig. 11 and Fig. 12. When we consider Coulomb effect which is neglected in our treatment and which will break the relation  $g_{nn} = g_{pp}$ , the much stronger screening effect for  $pp$  interaction leads to  $|g_{pp}| < |g_{nn}|$ . As a result,  $pp$  pairing will become further impossible to be in BEC state.

#### D. Phase Diagram in $\rho - \alpha$ Plane

The phase diagram of asymmetric nuclear matter in the  $\rho - \alpha$  plane at zero temperature is presented in Fig. 13. For  $\alpha = 0$  only  $\Delta_{np}$  could exist, and for  $\alpha = 1$  only  $\Delta_{nn}$  survives. These two limits have been discussed in III A and III B, and we will in this sub-section consider the phase structure in the region of  $0 < \alpha < 1$ .

Due to the mismatch between neutron and proton Fermi surfaces induced by the asymmetry  $\alpha \neq 0$ , there should be no  $np$  pairing when the mismatch is large enough. Since the coupling constant in  $I = 0$  channel is density independent and the pairing is dynamically controlled only by the in-medium mass, the critical asymmetry  $\alpha_{np}^1(\rho)$  for the BCS superfluid increases with decreasing density. When the system enters the superfluid state, the correlation becomes more and more strong with decreasing density and the system will go into the crossover region at a critical density defined by  $\xi_{np}/d = 1$ . When the density further decreases, the  $np$  pairing starts to be in the BEC state at another critical density defined by  $\mu = 0$ . Corresponding to the above two critical densities, the two boundaries of the BCS-BEC crossover in Fig. 13 are indicated respectively by  $\alpha_{np}^2(\rho)$  and  $\alpha_{np}^3(\rho)$ . At higher asymmetry,  $\alpha_{np}^1$  and  $\alpha_{np}^2$  coincide and the nuclear matter goes directly from the normal state into the strongly correlated superfluid.

Different from the  $I = 0$  channel, the pairing in  $I = 1$  channel has no Fermi surface mismatch and the superfluid can survive at any asymmetry when the density is not high enough. In Fig. 13 the  $I = 1$  superfluid exists in the whole  $\rho - \alpha$  plane. As we mentioned above, at  $\alpha = 0.1$  the critical density for  $nn$  pairing to go into the strongly coupled region is larger than the one for  $pp$  pairing. This is true for any asymmetry. In Fig. 13 the boundary  $\alpha_{nn}^2(\rho)$  defined by  $\xi_{nn}/d_n = 1$  for  $nn$  pairing is always on the right-hand side of the one  $\alpha_{pp}^2(\rho)$  defined by  $\xi_{pp}/d_p = 1$  for  $pp$  pairing. It is interesting that

the critical density for  $nn$  pairing is almost a constant for any asymmetry. There is no room for the BEC state of  $nn$  or  $pp$  pairing at any asymmetry  $0 \leq \alpha \leq 1$ .

Note that there exist three jumps in the phase diagram. The jump from normal state at  $\rho = 0$  to the  $np$  pairing BEC state at  $\rho \neq 0$ , the jump from  $np$  pairing at  $\alpha = 0$  to the  $np$ ,  $nn$  and  $pp$  pairings at  $\alpha \neq 0$ , and the jump from  $nn$  pairing at  $\alpha = 1$  to  $np$ ,  $nn$  and  $pp$  pairings at  $\alpha < 1$ .

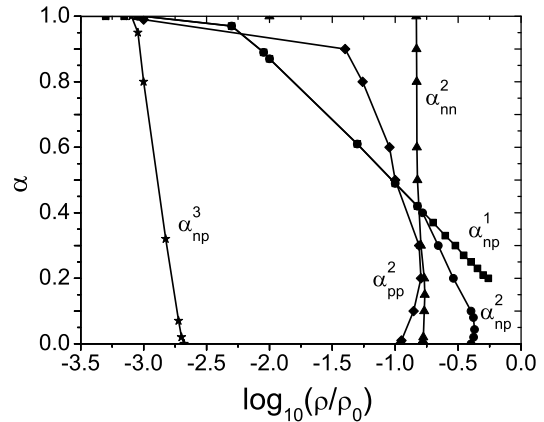


FIG. 13: The phase diagram for asymmetric nuclear matter in  $\rho - \alpha$  plane at zero temperature.  $\alpha_{np}^1$  is the critical asymmetry for  $np$  pairing BCS superfluid,  $\alpha_{np}^2$  and  $\alpha_{np}^3$  are the two boundaries of  $np$  pairing BCS-BEC crossover, and  $\alpha_{nn}^2$  ( $\alpha_{pp}^2$ ) is the boundary for  $nn$  ( $pp$ ) pairing to enter the strongly coupled region.

#### IV. THERMODYNAMICS AT HIGH DENSITY

The Cooper pairs could be broken by both large mismatch between the Fermi surfaces of the partner nucleons and large thermal fluctuation. The former is characterized by the asymmetry  $\alpha$ , and the latter is described by temperature  $T$ . We in this section examine the thermal and asymmetric effect on the nuclear matter in weak coupling region, *i.e.*, in the BCS region where the mean field analysis is still reliable. From the above calculation at zero temperature, this region is around and below the normal nuclear density  $\rho_0$ . Our purpose is to determine the phase diagram in  $\alpha - T$  plane at a fixed density.

We must emphasize that the asymmetry may lead to the so-called phase separating instability, which means that the ground state may favor the spatial separation of different phases. To study such an instability we define the nuclear density susceptibility matrix  $\chi$  with elements  $\chi_{ij} = \partial\mu_i/\partial\rho_j$  with  $i, j = n, p$ . For an uniform matter,  $\chi$  is always positively defined, and  $\chi < 0$  can be used as an indication of the appearance of phase separation (One should note that  $\chi < 0$  is only a necessary but not sufficient condition for the occurrence of phase separation). In the following discussion the term phase separation is refer to the state with  $\chi < 0$ . In a

practical manner,  $\chi$  can be computed through [40]

$$\begin{aligned}\chi_{ij} &= -\left.\frac{\partial^2 \mathcal{F}}{\partial \rho_i \partial \rho_j}\right|_{\rho} \\ &= -\left.\frac{\partial^2 \Omega}{\partial \mu_i \partial \mu_j}\right|_{\mu} + Y_i R^{-1} Y_j^\dagger\end{aligned}\quad (21)$$

with

$$\begin{aligned}Y_i &= \left( \left.\frac{\partial^2 \Omega}{\partial \mu_i \partial \Delta_{nn}}\right|_{\mu}, \left.\frac{\partial^2 \Omega}{\partial \mu_i \partial \Delta_{pp}}\right|_{\mu}, \left.\frac{\partial^2 \Omega}{\partial \mu_i \partial \Delta_{np}}\right|_{\mu}, \left.\frac{\partial^2 \Omega}{\partial \mu_i \partial q}\right|_{\mu} \right), \\ R &= \begin{pmatrix} \frac{\partial^2 \Omega}{\partial \Delta_{nn}^2} & \frac{\partial^2 \Omega}{\partial \Delta_{nn} \partial \Delta_{pp}} & \frac{\partial^2 \Omega}{\partial \Delta_{nn} \partial \Delta_{np}} & \frac{\partial^2 \Omega}{\partial \Delta_{nn} \partial q} \\ \frac{\partial^2 \Omega}{\partial \Delta_{pp} \partial \Delta_{nn}} & \frac{\partial^2 \Omega}{\partial \Delta_{pp}^2} & \frac{\partial^2 \Omega}{\partial \Delta_{pp} \partial \Delta_{np}} & \frac{\partial^2 \Omega}{\partial \Delta_{pp} \partial q} \\ \frac{\partial^2 \Omega}{\partial \Delta_{np} \partial \Delta_{nn}} & \frac{\partial^2 \Omega}{\partial \Delta_{np} \partial \Delta_{pp}} & \frac{\partial^2 \Omega}{\partial \Delta_{np}^2} & \frac{\partial^2 \Omega}{\partial \Delta_{np} \partial q} \\ \frac{\partial^2 \Omega}{\partial q \partial \Delta_{nn}} & \frac{\partial^2 \Omega}{\partial q \partial \Delta_{pp}} & \frac{\partial^2 \Omega}{\partial q \partial \Delta_{np}} & \frac{\partial^2 \Omega}{\partial q^2} \end{pmatrix}.\end{aligned}\quad (22)$$

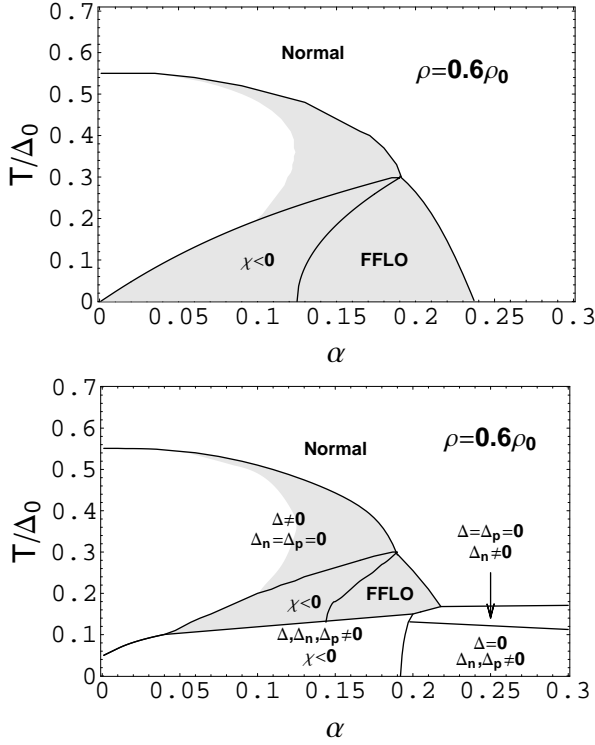


FIG. 14: The phase diagram of a mismatched nuclear superfluid at fixed nuclear density  $\rho/\rho_0 = 0.6$  in  $\alpha - T$  plane. The upper panel is for the familiar superfluid with only  $I = 0$  pairing, and in the lower panel the  $I = 1$  pairing is included as well. The shadowed regions indicate the gapless superfluid.  $\Delta_0 = 7.7$  MeV is the condensate in  $I = 0$  channel at  $\alpha = 0$  and  $T = 0$ .

By calculating the coupled gap and number equations at finite temperature, we obtain all the possible homogeneous phases and inhomogeneous FFLO phase. From the comparison of their free energies, we then extract the lowest one at fixed  $\rho$ ,  $\alpha$  and  $T$ . Finally we investigate the stability of the system against the number fluctuations by computing the number susceptibility matrix  $\chi$ , the state with non positive-definite

$\chi$  may be a phase separation. In Fig. 14 we show the phase diagram in  $\alpha - T$  plane at fixed nuclear density  $\rho/\rho_0 = 0.6$ .

The phase diagram without  $I = 1$  pairing is presented in the upper panel. The system is in normal state when the asymmetry or temperature is high enough, and the superfluid is in homogeneous state at high temperature and FFLO state at low temperature. However, the number susceptibility in the region of low temperature and low number asymmetry is not positive-definite, the FFLO state in this region is therefore unstable against the number fluctuations, and the ground state is probably an inhomogeneous mixture of the BCS superfluid and normal nuclear fluid. The shadowed region is the gapless superfluid with  $\delta\mu > \Delta_{np}$  where the energy gap to excite quasi-nucleons is zero and the system may be sensitive to the thermal and quantum fluctuations.

The phase diagram with both  $I = 0$  and  $I = 1$  pairings is shown in the lower panel of Fig. 14. Besides the familiar phase with only  $I = 0$  pairing ( $\Delta_{np} \neq 0, \Delta_{nn} = \Delta_{pp} = 0$ ) and the expected phases with only  $I = 1$  pairing ( $\Delta_{nn}, \Delta_{pp} \neq 0, \Delta = 0$  and  $\Delta_{nn} \neq 0, \Delta_{np} = \Delta_{pp} = 0$ ), there appears a new phase where the two kinds of pairings coexist ( $\Delta_{np}, \Delta_{nn}, \Delta_{pp} \neq 0$ ). In this new phase the FFLO momentum is zero and the number susceptibility is negative,  $\chi < 0$ . Therefore, the homogeneous superfluid in this region is unstable against number fluctuations, and the ground state is probably an inhomogeneous mixture of these three superfluid components. In the familiar phase with only  $I = 0$  pairing, there remains a stable FFLO region and an unstable FFLO triangle where the number susceptibility is negative and the system may be in the phase separation of the BCS superfluid and normal nuclear fluid. The gapless state appears only in the  $I = 0$  pairing superfluid, and in the region with  $I = 1$  pairing all the nucleons are fully gapped. Since the Fermi surface for  $nn$  pairing is higher than the one for  $pp$  pairing, the critical temperature to melt the  $nn$  condensate is higher than that for melting the  $pp$  condensate, and the difference between the two increases with increasing asymmetry.

## V. SUMMARY

We have investigated the phase structure of isospin asymmetric nuclear superfluid with pairings in both  $I = 0$  and  $I = 1$  channels in the frame of the density dependent contact potential. We calculated at zero temperature and in mean field approximation the pair wave functions, pair condensates, nucleon chemical potentials and effective couplings which are normally considered as characteristic quantities describing BCS-BEC crossover, and found that in general asymmetric nuclear matter only the  $np$  pair could form true bound state at extremely low density, and  $nn$  and  $pp$  pairs, on the other hand, could never form bound state at any density and asymmetry. We also studied the phase diagram for weakly coupled nuclear superfluid at finite temperature. Since the attractive interaction for  $I = 1$

pairing is weaker than the one for  $I = 0$  pairing, the inclusion of  $nn$  and  $pp$  pairings changes significantly the conventional phase diagram with only  $np$  pairing only at low temperature. For systems with fixed nuclear density, the two kinds of pairings can coexist at low temperature and low number asymmetry. By calculating the number susceptibility, this new phase is not in the FFLO state but probably an inhomogeneous mixture of the  $np$ ,  $nn$  and  $pp$  superfluid components. In any region with  $I = 1$  pairing, the interesting gapless superfluid is washed out and all quasi-nucleons are fully gapped.

**Acknowledgments:** X.H. thanks A.Sedrakian for helpful discussions. The work is supported by the NSFC Grant 10735040 and the National Research Program Grants 2006CB921404 and 2007CB815000.

- 
- [1] A. L. Goodman, Phys. Rev. **C58**, R3051 (1998).
  - [2] A. L. Goodman, Phys. Rev. **C60**, 014311 (1999).
  - [3] M. Baldo, U. Lombardo and P. Schuck, Phys. Rev. **C52**, 975 (1995).
  - [4] D. Blaschke, N. K. Glendenning and A. Sedrakian, Eds., *Physics of neutron star interiors*. Proceedings, ECT International Workshop, NSF'00, Trento, Italy, June 19-July 6, 2000, Lect. Notes Phys.58712001.
  - [5] A. Sedrakian, Prog. Part. Nucl. Phys. **58**, 168 (2007), and references there in.
  - [6] T. Alm, *et al.*, Nucl. Phys. **A551**, 45 (1993).
  - [7] U. Lombardo, *et al.*, Phys. Rev. **C64**, 064314 (2001).
  - [8] A. A. Isayev, S. I. Bastrukov and J. Yang, Nucl. Phys. **A734**, E112 (2004); Phys. Atom. Nucl. **67**, 1840 (2004).
  - [9] A. A. Isayev, JETP. Lett. **82**, 551 (2005).
  - [10] A. A. Isayev, Phys. Rev. **C78**, 014306 (2008).
  - [11] M. Matsuo, Phys. Rev. **C73**, 044309 (2006).
  - [12] K. Hagino, *et al.*, Phys. Rev. Lett. **99**, 022506 (2007) and the comment by N. T. Zinner and A. S. Jensen, Phys. Rev. Lett. **101**, 179201 (2008) and the reply by K. Hagino, *et al.*, Phys. Rev. Lett. **101**, 179202 (2008).
  - [13] J. Margueron, H. Sagawa and K. Hagino, Phys. Rev. **C76**, 064316 (2007).
  - [14] A. J. Leggett, in *Modern trends in the theory of condensed matter*, edited by A. Pekalski and R. Przystawa, Springer-Verlag, Berlin, 1980.
  - [15] P. Nozières and S. Schmitt-Rink, J. Low. Temp. Phys. **59**, 195(1985).
  - [16] C. A. R. Sá de Melo, M. Randeria and J. R. Engelbrecht, Phys. Rev. Lett. **71**, 3202 (1993).
  - [17] A. Sedrakian and U. Lombardo, Phys. Rev. Lett. **84**, 602 (2000).
  - [18] A. I. Akhiezer, *et al.*, Phys. Rev. **C63**, 021304 (2001).
  - [19] A. Sedrakian, Phys. Rev. **C63**, 025801 (2001).
  - [20] H. Muther and A. Sedrakian, Phys. Rev. **C67**, 015802 (2003).
  - [21] M. Alford, G. Good and S. Reddy, Phys. Rev. **C72**, 055801 (2005).
  - [22] M. Jin, L. He and P. Zhuang, arXiv: nucl-th/0609065.
  - [23] G. Sarma, J. Phys. Chem. Solids **24**, 1029 (1963).
  - [24] W. Liu and F. Wilczek, Phys. Rev. Lett. **90**, 047002 (2003).
  - [25] P. Fulde and R. Ferrel, Phys. Rev. **A135**, 550 (1964); A. Larkin and Y. Ovchinnikov, Sov. Phys. JETP **20**, 762 (1965).
  - [26] H. Muther and A. Sedrakian, Phys. Rev. Lett. **88**, 252503 (2002).
  - [27] A. Sedrakian, *et al.*, Phys. Rev. **A72**, 013613 (2005).
  - [28] P. Bedaque, H. Caldas and G. Rupak, Phys. Rev. Lett. **91**, 247002 (2003).
  - [29] H. Caldas, Phys. Rev. **A69**, 063602 (2004).
  - [30] E. Garrido, *et al.*, Phys. Rev. **C60**, 064312 (1999); **63**, 037304 (2001).
  - [31] J. F. Berger, M. Girod and D. Gogny, Comp. Phys. Comm. **63**, 365 (1991).
  - [32] P. Ring and P. Schuck, *The Nuclear Many Body Problem*, Springer-Verlag, New York, 1980.
  - [33] J. Dechargé and D. Gogny, Phys. Rev. **C21**, 1568 (1980).
  - [34] I. M. Khalatnikov, JETP. Lett. **17**, 386 (1973); V. Mineev, Sov. Phys. JETP **40**, 132 (1974).
  - [35] D. E. Sheehy and L. Radzihovsky, Phys. Rev. Lett. **96**, 060401 (2006).
  - [36] H.Muther and W.H.Dickhoff, Phys. Rev. **C72**, 054313(2005).
  - [37] J. Bardeen, L. N. Cooper and J. R. Schrieffer, Phys. Rev. **108**, 1175(1957).
  - [38] J. Friedel, Adv. Phys. **3**, 446(1954).
  - [39] J.Kapusta and T.Toimela, Phys. Rev. **D37**, 3731(1988); J.Diaz-Alosa, A.Perez Canyellas and H.Sivak, Nucl. Phys. **A505**, 695(1989); J.Durso, H.Kim and J.Wambach, Phys. Lett. **B298**,267(1993); J.Diaz-Alosa, E.Gallego and A.Perez, Phys. Rev. Lett.**73**, 2536(1994); H.Sivak, A.Perez and J.Diaz-Alonso, Prog. Ther. Phys. **105**, 961(2001); E.Epelbaum, Prog. Part. Nucl. Phys. **57**, 654(2006); Ch.Mu and P.Zhuang, Eur. Phys. J. **C58**, 271(2008).
  - [40] X. G. Huang, X. W. Hao and P. F. Zhuang, New J. Phys. **9**, 375 (2007); Int. J. Mod. Phys. **E16**, 2307 (2007).